Discharge-Mode Testing of the X-EPT Microwave ECR Gridded Ion Thruster

IEPC-2019-652

David Hoffman[1] and Angelo Grubišić
Faculty of Engineering and Physical Sciences, University of Southampton, Southampton, Hampshire, SO17 1BJ,
United Kingdom

Abstract: **A low-cost, 20-cm-diameter microwave electron cyclotron resonance ion thruster (Xenon Electric Propulsion Thruster, XEPT) has been built and tested in discharge-only mode to investigate the suitability of the technology for commercial satellite missions. Thruster design makes use of selective laser melting, a metal additive manufacturing technique, and off-the-shelf components wherever possible. This includes a 2.45 GHz solid-state microwave generator and a magnetic circuit formed by small, samarium cobalt and neodymium magnets. These two magnetic materials were tested in two layouts in combination with end-wall and side-wall propellant (argon) injection ports. The preliminary aim of the XEPT project is to achieve 80% of the performance of the μ20 thruster in terms of ion production cost and mass utilisation efficiency. The current version of XEPT met the stated ion production cost target but did not yet reach the stated mass utilisation efficiency target.**

Nomenclature

B	=	magnetic flux density
e	=	electron charge
ε_0	=	permittivity of free space
$\vec{E}$	=	microwave electric field vector
m_e	=	electron mass
n_e	=	electron (plasma) density
n_{crit}	=	cut-off (critical) plasma density
ω_c	=	electron angular gyro-frequency
ω	=	microwave angular frequency
ω_p	=	plasma frequency

I.   Introduction

MICROWAVE discharge ion thrusters, which produce plasma by electron cyclotron resonance (ECR) heating are a potentially attractive propulsion option for commercial missions as they offer many distinct advantages over DC and even RF ion thrusters:

---

[1] PhD student, Aeronautics and Astronautics, d.hoffman@soton.ac.uk

- Complete elimination of hollow cathodes and associated lifetime and contamination issues.
- Simplified electrical architecture with no heavy, high current power lines, fewer power supplies [1] and generally less physical wiring susceptible to radiation damage [2].
- Option to use less expensive, lower purity xenon since cathode poisoning is no longer a concern, yielding considerable cost savings [2].
- Simplified ion optics design and reduced localised grid wear due to more uniform plasma density [2].
- Longer screen grid life due to reduced sputter erosion of the upstream surface (lower plasma potential) [2].
- Longer accel grid life due to uniform electron back-streaming limit across the grid area [2].
- High reliability as demonstrated by the 10-cm-diameter μ10 thrusters on the Hayabusa asteroid sample return missions [3]

Leveraging these advantages for commercial satellite applications drove the development of Xenon Electric Propulsion Thruster (XEPT), a low-cost, microwave discharge ion thruster in the sub-kilowatt range. The thruster design makes use of additive manufacturing and off-the-shelf components wherever possible to avoid customised components as these may represent prohibitive costs for commercial operators with a limited budget. As opposed to the JAXA μ ("mu") thruster series, which operate at a frequency of 4.25 GHz [4], XEPT operates at a standard frequency of 2.45 GHz, eliminating highly customised microwave generation and transmission, which greatly reduces system. To further reduce cost, the magnetic circuit used for plasma production and confinement is composed of a large number of commercially stocked, cylindrical permanent magnets arranged in rings in contrast to bespoke, solid magnet rings of the μ thrusters [5]. The preliminary aim of the XEPT project is to achieve 80% of the performance of the μ20 thruster, in line with the general principle of 80/20 adopted by satellite manufacturers such as Surrey Satellite Technology Limited (SSTL). This paper will present the design of XEPT and discharge-mode test results for two configurations of propellant ports (end-wall, side-wall) and two configurations of magnetic circuit layouts employing samarium cobalt (SmCo) and N45SH neodymium (NdFeB) magnets.

II.   Background

Microwave discharge ion thrusters utilise a cathode-less mechanism known as electron cyclotron resonance (ECR) to generate primary electrons, which then ionise propellant. The ECR effect heats up magnetised thermal electrons by directly transferring microwave energy into electron gyro-motion. In "resonance zones" where the electron gyro-frequency equals the microwave angular frequency, $\omega_c = eB/m_e = \omega$, electrons are accelerated by the component of the induced electric field that is parallel to electron tangential (rotational) direction. This wave-particle interaction dampens the electromagnetic wave and increases the total electron kinetic energy, manifesting itself as an increase in electron Larmor radius. Electrons are magnetically trapped within a magnetic mirror, gaining sufficient energy by crossing the resonance zones before undergoing ionising collisions with atoms. ECR is an efficient method of electron heating until plasma reaches a density limit n_{crit} at which point microwaves start getting reflected back into the transmission circuit. This is known as the cut-off condition, which occurs when the plasma frequency ω_p, related to free electron oscillation in the plasma, exceeds the microwave angular frequency:

$$\omega_p = \sqrt{\frac{e^2 n_e}{\varepsilon_0 m_e}} \geq \omega. \tag{1}$$

The cut-off density limit thus scales quadratically with the microwave frequency. At 2.45 GHz, the magnetic flux density required for ECR is $B = 87.5$ mT and the cut-off density limit is $n_{crit} = 7.45 \times 10^{16} m^{-3}$.

III.   X-EPT Ion Source Design

The design of the ion source was remotely based on that of the fourth (IV) version of the μ20 thruster [4]. Figure 1 shows two images of the 20-cm-diameter, stainless steel discharge chamber, additively manufactured as a single component using selective laser melting. Cylindrical SmCo and/or NdFeB permanent magnets, shown as white circles in the Figure 1a), were slotted individually into the built-in housing. The housing consists of 136 magnets, 10 mm in diameter and 7.5 mm tall, arranged in four rings with two additional magnets on opposing sides forming "magnetic bridges" to enable $\vec{E} \times \vec{B}$ and $\nabla \vec{B}$ electron drifts into the outer regions of the chamber. The spacing between the two innermost magnet rows is twice that of the other rows. This results in a weaker magnetic field, which reduces microwave power absorption in the innermost plasma ring enabling wave propagation to the outer

2

regions [4]. The slots in the magnet housing taper slightly at the top to hold the magnets in position. A quarter-wave, monopole antenna with a Macor ceramic sleeve is placed in the centre of the chamber for protection against contamination and multipactor discharge. Propellant is directly injected into the chamber via eight ports, four on the end wall (base) and four on the side walls. The ports on the base are arranged in a straight line as it was previously shown that this configuration produces higher ion currents albeit with worse beam flatness relative to a circular configuration [5]. The side-wall ports are evenly spaced and offset by 45 degrees from the magnetic bridges.
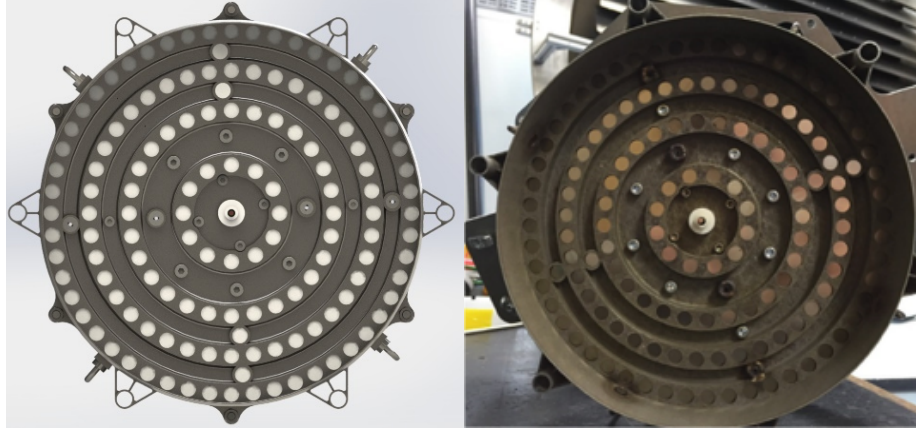

Figure 1. a) Rendered CAD image of the discharge chamber b) Image of the additively manufactured discharge chamber prototype

IV.   Discharge-Mode Testing

A. Test setup

Testing was conducted in the David Fearn Electric Propulsion Laboratory at the University of Southampton. Pressure in the chamber was monitored by a Pfeiffer Vacuum PKR 251 gauge with a Pirani sensor and an inverted magnetron cold cathode gauge. The ensemble of roughing and turbo-molecular pumps can achieve a pressure of 1 x 10^{-6} mbar with no gas inflow and can maintain a pressure of 3 x 10^{-5} to 7 x 10^{-5} mbar when low flow rates (0 – 10 SCCM) are used. Figure 2 shows the schematic of the discharge-mode test setup and the electrical, fluidic and microwave ground support equipment. Ions generated by microwave discharge were drawn to an ion collector plate. The ion collector was photochemically etched from a 1mm-thick stainless steel plate and mounted on the discharge chamber at three mounting points. The collector was electrically isolated from the chamber using Macor bushings shielded from deposition of sputtered material by steel caps. The collector was operated in voltage-controlled mode at -30 V by a commercial power supply, Kikusui PWX750MHF. A Keysight Technologies 34401A six-digit multimeter was connected in series with the power supply and the collector to measure the extracted ion current. All in-vacuum wiring was Kapton-insulated. Microwaves were fed into the thruster by a 7/16 DIN coaxial cable connected to a Wattsine 2.45 GHz solid-state microwave generator. A triple-stub tuner installed on the waveguide network was used in conjunction with a reflected microwave power detector for impedance matching. The discharge chamber was grounded by the outer conductor of the coaxial cable. It was not necessary to isolate the thruster from ground for discharge mode testing. Argon gas was used as propellant instead of xenon to reduce the cost of testing. Gas was drawn at 10 bar from a pressurized cylinder and fed into a Bronkhorst F-201-CV-050 mass flow controller (MFC) at a pressure of 4 bar using a regulator. Mass flow rate downstream of the MFC can be varied from 0 to 40 SCCM using the FlowView software on a local PC. A system of valves mounted on the outside of the vacuum chamber allowed manual control of the gas flow into each of the four pairs of gas ports: inner and outer end-wall ports and the two opposing pairs of side-wall ports.
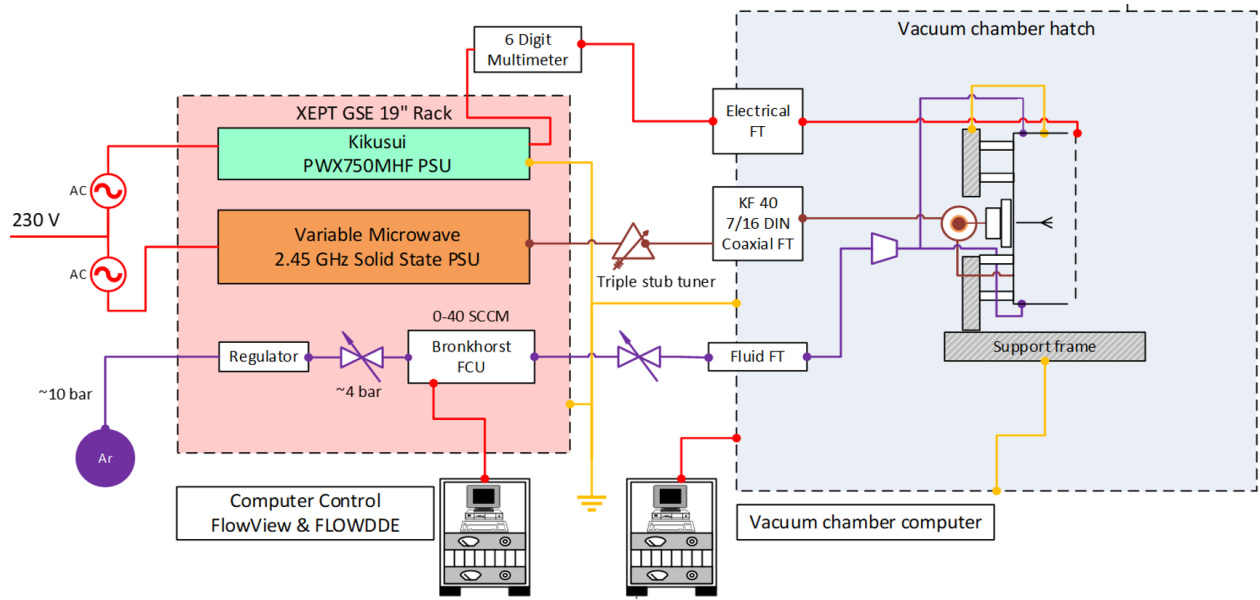
Figure 2. Schematics of the ground support equipment and experimental setup

B. Test results

Plasma ignited at flow rate ranging from 3 to 6 SCCM and forward microwave power range of 30 to 60 W. Instabilities such as disappearance of plasma regions or high sudden reflected power occured at flow rates less than 3 SCCM and at low microwave power levels (<40 W) when high flow rates were used (>8 SCCM). Two injector layouts were tested: side-wall ports, and end-wall ports and two magnetic circuit layouts: 1) SmCo magnets in all rings, and 2) SmCo magnets in the innermost ring with NdFeB magnets in the three outer rings. As shown in Figures 3 and 4, ion current sharply rose between 30 W and 70 W for all tested flow rates. Beyond 70 W, there were only minor increases in ion current as the microwave power was increased up to 120 W. The highest ion currents were: 279 mA (3a), 292 mA (3b), 284 mA (4a), 286 mA (4b). These were achieved at 8 SCCM in all cases except in 4b, which was achieved at 10 SCCM. With the N45SH magnets, it was possible to sustain plasma in all rings even at 20 W while when the SmCo magnets were used, the inner plasma ring disappeared at less than 40 W (shown in Figure 7, Appendix).
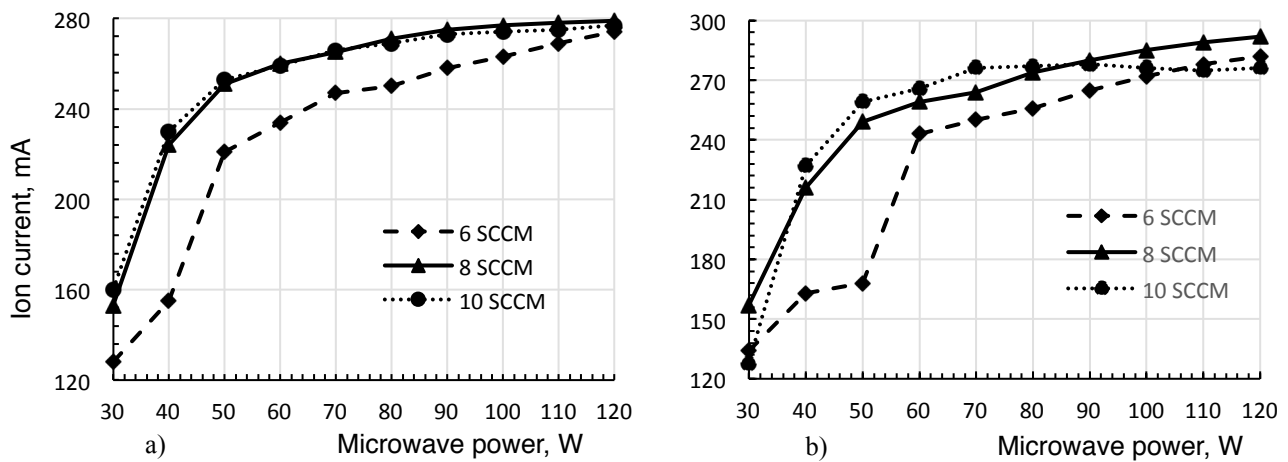

Figure 3. Ion current extracted by the ion collector plate as a function of microwave power with a) end-wall propellant injection b) side-wall propellant injection. SmCo in the innermost ring; NdFeB magnets elsewhere.

4

Figure 5 depicts the performance curves of XEPT. Curves marked "NdFeB" refer to those magnetic circuit layouts where the innermost magnet ring was made up of SmCo magnets while the three outer rings were made up of NdFeB magnets. Curves marked "SmCo" refer to those magnetic circuit layouts where all magnets were SmCo. As shown in Figure 5a), ion production cost spiked notably between 30-40% mass utilisation efficiencies for all tested configurations. Performance curves reached their optimal operating point (i.e. the "knee") at 51-57% mass utilisation efficiency and 226 – 329 W/A ion production cost before commencing a steady linear growth as efficiency further increased. At 8 SCCM, ion production cost remained fairly constant as utilisation efficiency increased from 25% to 45%. The optimal operating points occured at 43-45% and 200-280 W/A ion production cost. On the other hand, as can be seen in Figure 6, the optimum operating point of the µ20 is at 72-73% mass utilisation efficiency and 226-244 W/A ion production cost for 8.6 and 9.6 SCCM. This is due to reasons, which inevitably increase the cost of the thruster: higher operating frequency and stronger magnetic circuit. The cut-off plasma density limit is proportional to the square of the microwave frequency, therefore the µ20 can create much denser plasma, leading to higher extracted ion current density. The µ20 also features a magnetic circuit composed of four solid axially magnetised rings [5] as opposed to a large number of small cylindrical magnets arranged in rings. The magnetic field in the µ20 is thus much stronger than that in XEPT, resulting in better electron confinement and lower discharge loss. Moreover, the magnetic circuit of the µ20 is held by virtue of magnetic attraction to a ferrous yoke plate, which eliminates the need for a physical magnetic housing and further enhances magnetic properties.
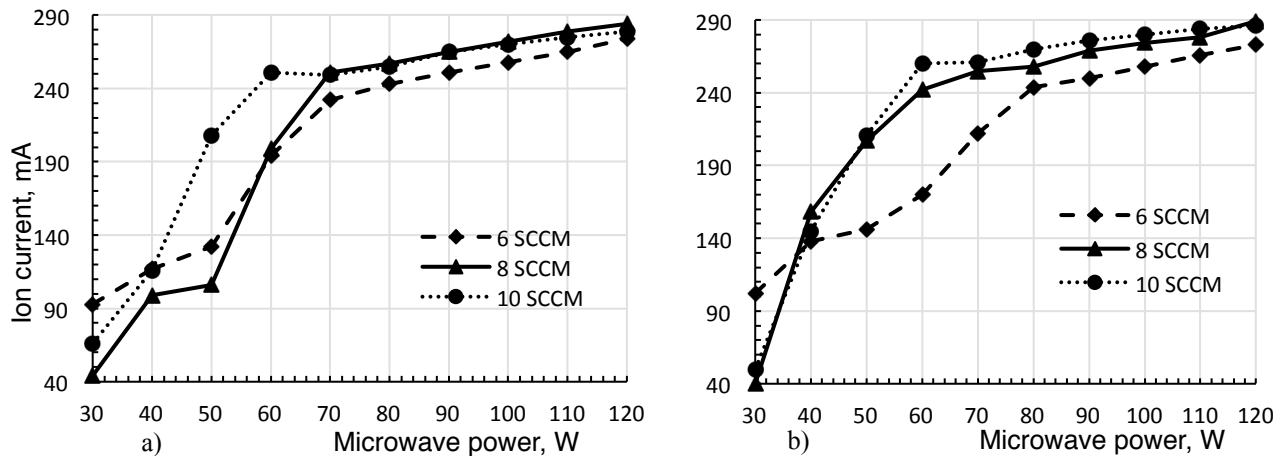

Figure 4. Ion current extracted by the ion collector plate as a function of microwave power with a) end-wall propellant injection and b) side-wall propellant injection. SmCo magnets in all four rings.
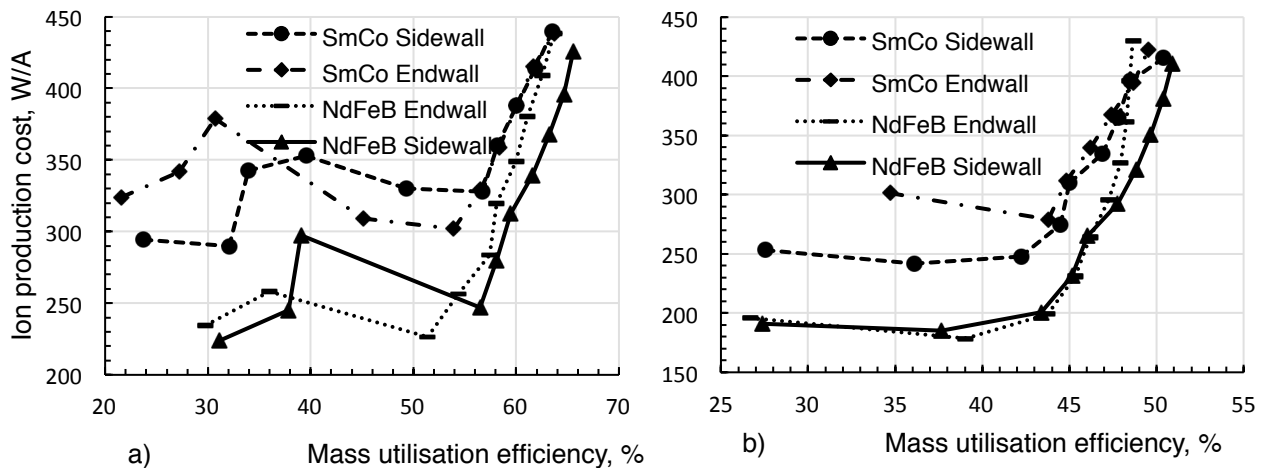

Figure 5. Performance curve of XEPT at a) 6 SCCM and b) 8 SCCM

5

Both of these attributes of the μ20 reduce electron wall losses and improve discharge efficiency.

V. Conclusion

A low-cost, 20-cm-diameter microwave discharge ion thruster made from additively manufactured and off-the-shelf components has been tested in discharge-only mode to measure its performance in the context of the μ20 thruster developed by JAXA. The current version of XEPT generally met the stated performance target in terms of ion production cost but not yet in terms of mass utilization efficiency. In the future, efforts will be made to increase thruster performance without incurring significant additional cost. For example, the physical magnet housing comprising of additively manufactured slots can be replaced by a yoke made from a ferrous material such as mild steel or annealed soft iron.
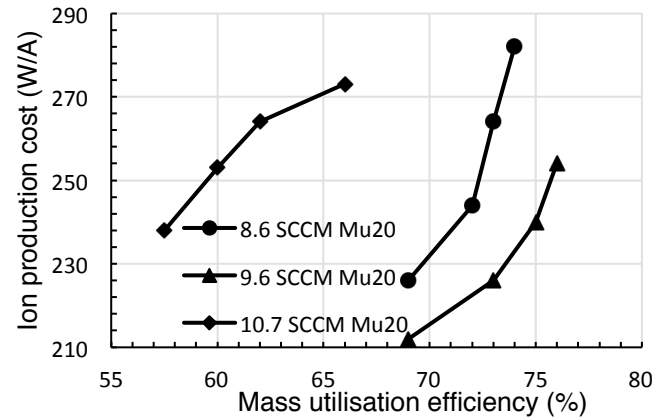

Figure 6. a) Performance curve of μ20 [5]

Acknowledgments

The author, David Hoffman, would like to dedicate this paper to his PhD supervisor, Dr. Angelo Grubišić, who tragically died in a BASE jump accident shortly before this IEPC.
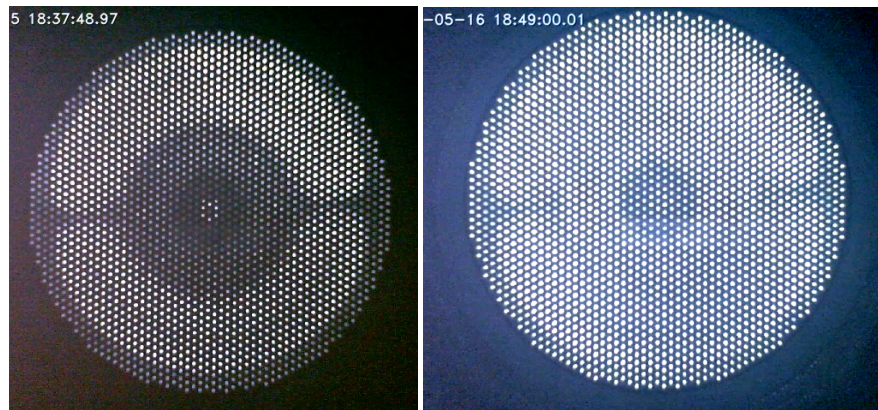
Appendix

Figure 7. XEPT a) Disappearance of the inner plasma ring b) Full plasma discharge

References

[1]   I. Funaki, K. Nishiyama, H. Kuninaka, H. Toki, K. Toki, and Y. Shimizu, "20mN-class Microwave Discharge Ion Thruster," in *27th International Electric Propulsion Conference*, 2001, p. 1.
[2]   J. E. Foster, H. Kamhawi, T. Haag, C. Carpenter, and G. Williams, "High Power ECR Ion Thruster Discharge Characterization," in *29th International Electric Propulsion Conference*, 2005, pp. 1–4.
[3]   G. Coral, R. Tsukizaki, K. Nishiyama, and H. Kuninaka, "Microwave power absorption to high energy electrons in the ECR ion thruster," *Plasma Sources Sci. Technol.*, vol. 27, no. 9, p. 1, 2018.
[4]   K. Nishiyama, H. Kuninaka, Y. Shimizu, and K. Toki, "30mN-class Microwave Discharge Ion Thruster," in *28th International Electric Propulsion Conference*, 2008, pp. 7–10.
[5]   K. Nishiyama, Y. Shimizu, H. Kuninaka, T. Miyamoto, M. Fukuda, and T. Nakail, "Research and Development Status of Microwave Discharge Ion Thruster μ20," in *29th International Electric Propulsion Conference*, 2005, pp. 3–5.